A Family of Invariant Stress Surfaces

Krenk, S.

Publication date:
1994

Document Version
Publisher's PDF, also known as Version of record

INSTITUTTET FOR BYGNINGSTEKNIK
DEPT. OF BUILDING TECHNOLOGY AND STRUCTURAL ENGINEERING
AALBORG UNIVERSITETSCENTER • AUC • AALBORG • DANMARK

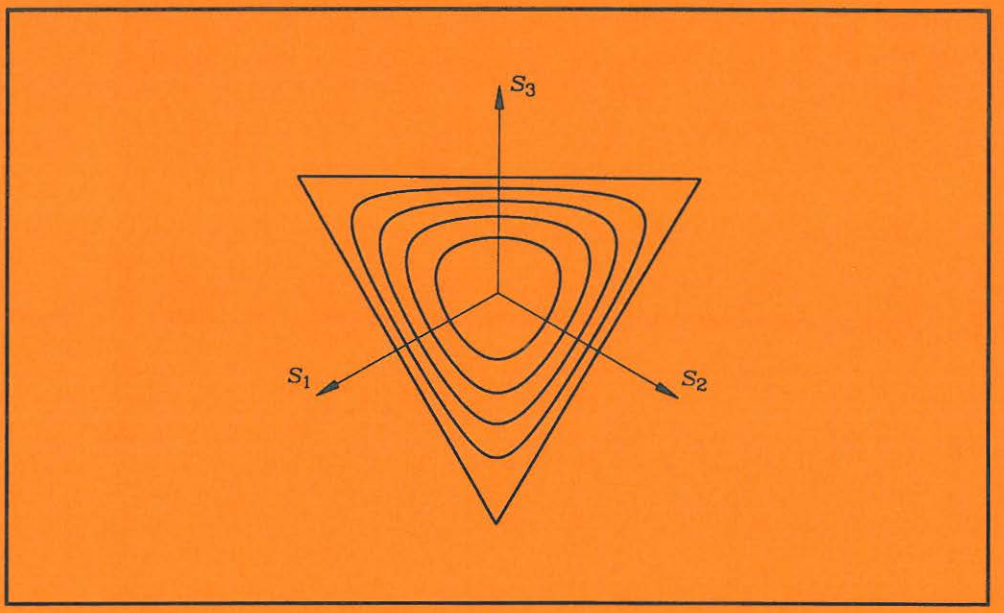

ENGINEERING MECHANICS
PAPER NO. 22

S. KRENK
A FAMILY OF INVARIANT STRESS SURFACES
FEBRUARY 1994 ISSN 0902-7513 R9402

The ENGINEERING MECHANICS papers are issued for early dissemination of research results from the Engineering Mechanics Group at the Department of Building Technology and Structural Engineering, University of Aalborg. These papers are generally submitted to scientific meetings, conferences or journals and should therefore not be widely distributed. Whenever possible, reference should be given to the final publications (proceedings, journals, etc.) and not to the Engineering Mechanics papers.

INSTITUTTET FOR BYGNINGSTEKNIK
DEPT. OF BUILDING TECHNOLOGY AND STRUCTURAL ENGINEERING
AALBORG UNIVERSITETSCENTER • AUC • AALBORG • DANMARK

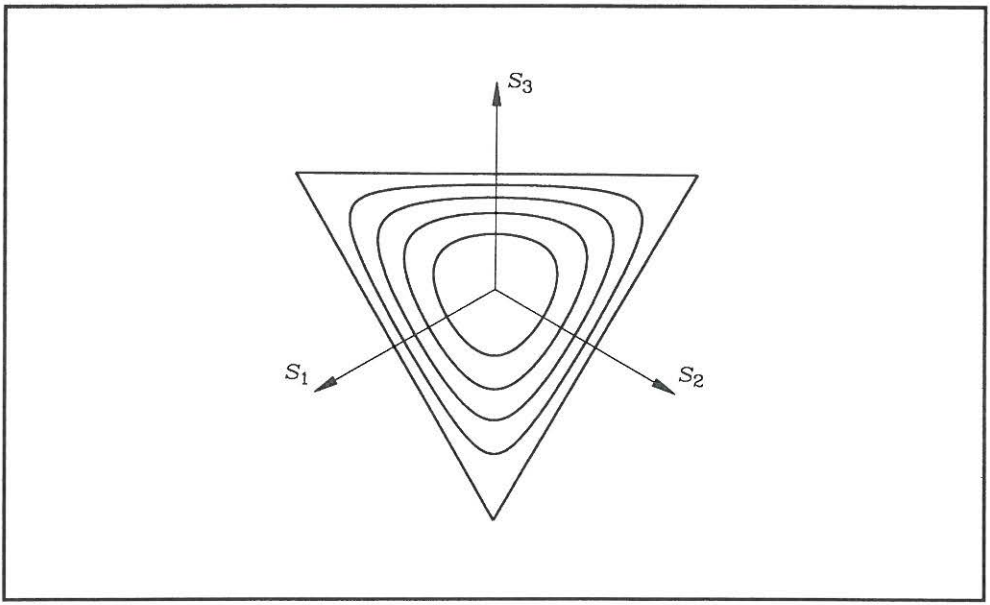

ENGINEERING MECHANICS
PAPER NO. 22

S. KRENK
A FAMILY OF INVARIANT STRESS SURFACES
FEBRUARY 1994 ISSN 0902-7513 R9402

A FAMILY OF INVARIANT STRESS SURFACES

STEEN KRENK
Department of Building Technology and Structural Engineering
Aalborg University, DK-9000 Aalborg, Denmark

Abstract

A family of invariant stress surfaces with a cubic dependence on the deviatoric stress components is expressed as a linear combination of the second and third deviatoric stress invariants. A simple geometric derivation demonstrates the convexity of the contours in the deviatoric plane. An explicit representation of the deviatoric contours in terms of a size and a shape parameter is given. The shape parameter effects a continuous transition from a triangle to a circle in the deviatoric plane. An explicit format in terms of the triaxial compresson and tension generators is derived, and the plane stress contour is given in explicit form. Several special cases are considered: a generalized Drucker-Prager criterion with straight generators and a smooth triangular deviatoric contour, surfaces with parabolic compression and tension generators, and the Lade failure surface for cohesionless soils. The use of an asymptotic tension cut-off condition in triaxial tension is discussed.

INTRODUCTION

Important properties such as failure and plastic deformation of solids is most often described in terms of surfaces in a space spanned by the stress components corresponding to a material point. These surfaces may serve as failure surface, yield surface or plastic potential. For isotropic materials these surfaces are usually described in invariant form, e.g. by use of the principal stress components $(\sigma_1, \sigma_2, \sigma_3)$. These invariant surfaces can be represented in a three-dimensional space of principal stresses, and must satisfy symmetry with respect to the three axes. In the description of real materials the mean stress

$$\sigma_m \;=\; \tfrac{1}{3}(\sigma_1 + \sigma_2 + \sigma_3) \tag{1}$$

plays a special role. It is therefore convenient to extract the mean stress and introduce the principal deviatoric stress components $s_1 = \sigma_1 - \sigma_m$, etc. . This is illustrated in Fig. 1, where the mean stress represents the component along the vector $(1,1,1)$, while the deviatoric stress components (s_1, s_2, s_3) are confined to a plane orthogonal to this vector.

The deviatoric stress components must appear in symmetric form. This is most easily accomplished by using the second deviatoric stress invariant

$$J_2 \;=\; \tfrac{1}{2}\left(s_1^2 + s_2^2 + s_3^2\right) \;=\; -\;(s_2 s_3 + s_3 s_1 + s_1 s_2) \tag{2}$$

and the third deviatoric stress invariant

$$J_3 \;=\; \tfrac{1}{3}\left(s_1^3 + s_2^3 + s_3^3\right) \;=\; s_1 s_2 s_3 \tag{3}$$

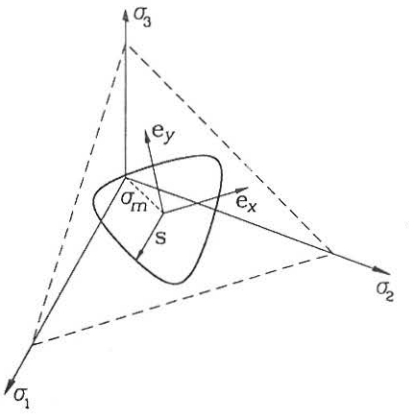

FIG. 1: Representation of stress space as mean stress and deviatoric plane.

In addition to preserving symmetry the use of σ_m, J_2 and J_3 permits direct evaluation i an arbitrary coordinate system by appeal to invariance. Thus the analysis of the surfac can be carried out using principal stress components, while the later use of the surface ca be made in terms of any convenient set of stress components.

For many metals the behavior in tension and compression is similar, and the main influenc on plasticity and failure is represented by J_2. This is reflected in the extensive use of th von Mises yield criterion, expressed entirely in terms of J_2. On the other hand the mea stress σ_m has a considerable influence on the behavior of granular materials. It is rathe simple to extend the von Mises surface to incorporate the mean stress, see e.g. Drucke & Prager (1952) and Bresler & Pister (1958). However, differences are often observe between the material behavior in triaxial compression, $\sigma_1 = \sigma_2 > \sigma_3$, and in triaxia tension $\sigma_1 > \sigma_2 = \sigma_3$. Representation of this difference requires the use of J_3. The simples stress surfaces including dependence on J_3 are those of Tresca and Mohr-Coulomb, whic assume independence of the intermediate principal stress component. These surfaces hav a hexagonal contour in any deviatoric plane, see e.g. Chen & Han (1988). They are mos easily described directly in terms of the principal stress components, but this and the lac of a unique normal at the corners make their use as yield surface and plastic potentia rather complicated.

The present paper describes a family of smooth surfaces given in terms of σ_m, J_2 an J_3. The format of these surfaces is a simple linear combination of the deviatoric stres invariants J_2 and J_3 with coefficients as arbitrary functions of the mean stress σ_m. Th deviatoric contours of this family of surfaces is a two-parameter family of curves with a siz parameter and a shape parameter that effects a transition form a circle to a triangle. Thu this family of invariant surfaces is determined uniquely by two generators, conveniently taken as the compression and the tension meridian.

The structure of the paper is as follows. First the general format of the deviatoric contours is described in terms of a size and a shape parameter, and a polar representation is given in the Appendix. It is then demonstrated how the size and shape parameters can be replaced explicitly by a triaxial compression and a triaxial tension stress. An explicit format for the plane stress contour is then presented. Finally three special cases are discussed: a generalized Drucker-Prager surface with linear generators and smooth triangular deviatoric contour, surfaces with parabolic compression and tension generators and their use as failure surfaces for concrete, and a special surface proposed by Lade for cohesionless soils.

THE DEVIATORIC CONTOURS

The simplest form a deviatoric contour that satisfies symmetry with respect to the three principal deviatoric stress components (s_1, s_2, s_3) is the cubic polynomial

$$(s_1 - c)(s_2 - c)(s_3 - c) \;=\; -\,\eta\, c^3 \tag{4}$$

where c is a parameter with dimension of stress and η is a non-dimensional parameter.

A geometric interpretation of the family of curves generated by (4) is shown in Fig. 2. For $\eta = 0$ the curve is composed of the three lines $s_j = c$, $j = 1, 2, 3$. The relevant part is the isosceles triangle corresponding to the midside points $s_1 = c$, $s_2 = s_3 = -\frac{1}{2}c$ etc., and the corner points $s_1 = -2c$, $s_2 = s_3 = c$. The product on the left side of (4) is a convex function taking values between zero at the triangle and c^3 at the center $s_1 = s_2 = s_3 = 0$. Any value of the parameter η in the interval 0 to 1 will therefore generate a symmetric convex curve. For small values of η the curve is nearly triangular, and for η close to 1 the curve approaches circular shape. The smooth transition from triangular to circular shape is illustrated in Fig. 2.

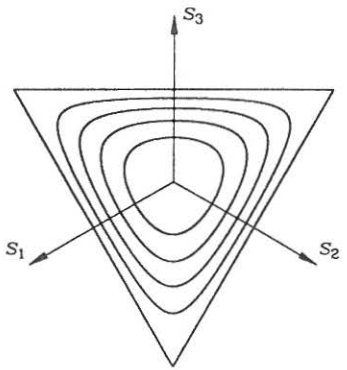

FIG. 2: Contour curves of cubic surface, $\eta = 0.0, 0.2, 0.4, 0.6, 0.8, 1.0$.

It is convenient to express the curves in terms of the deviatoric invariants J_2 and J_3. Wh
it is used that the sum of the deviatoric stresses is zero, the relation (4) takes the form

$$s_1 s_2 s_3 \; - \; c\,(s_2 s_3 + s_3 s_1 + s_1 s_2) \; = \; (1-\eta)\,c^3 \qquad (7)$$

and it follows immediately from (2) and (3) that this is

$$J_3 \; + \; c\,J_2 \; = \; (1-\eta)\,c^3 \qquad (8)$$

Thus, in any deviatoric plane the contour is given in terms of a size parameter c and a sha
parameter η. These parameters are not convenient in practice, because c is only indirect
related to the size of the contour via the shape parameter η. It is more convenient to u
a shape parameter γ and a size parameter s_0 defined by

$$\gamma^2 \; = \; 1 - \eta \quad , \quad s_0 \; = \; \gamma\, c \qquad (9)$$

This gives the relation the form

$$\frac{\gamma J_3}{s_0^3} \; + \; \frac{J_2}{s_0^2} \; = \; 1 \qquad (10)$$

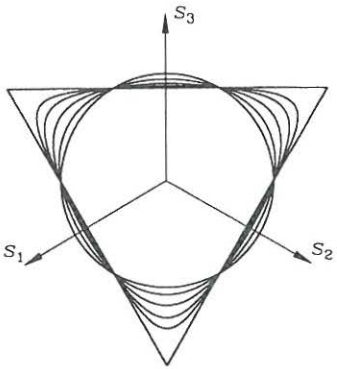

FIG. 3: Normalized cubic contour curves, $\gamma = 0.0, 0.3, 0.6, 0.8, 0.9, 1.0$.

The renormalized curves are shown in Fig. 3. The parameter s_0^2 is the value of the J_2 a
points where $J_3 = 0$, i.e. at points where one of the deviatoric stress components s_j vanish
These points correspond to triaxial shear, e.g. $s_1 = 0$, $s_2 = -s_3 = s_0$. There are 6 of thes
points on the contour in the deviatoric plane, located on lines inclined $\pm 30°$ with the thre
deviatoric axes. At these points the contours are independent of the shape parameter γ
and thus the size parameter s_0 is in fact a representative magnitude of the deviatoric stres
components. In (8) the size parameter s_0 can be taken as positive. It then follows fron
(7) that the shape parameter γ varies between 0 and ± 1, with small values correspondin

to nearly circular contours and values close to ± 1 giving nearly triangular shape. Positive values of γ correspond to the orientation of the triangle as shown in Figs. 2 and 3 with the corners located on the negative part of the s_j-axes. For negative value of γ the corners of the triangle would be loacated on the positive part of the s_j-axes, but this is of less interest in the description of actual material behaviour.

The contours (8) generate a surface in stress space, when the parameters s_0 and γ are considered as functions of the mean stress $\sigma_m = \frac{1}{3}(\sigma_1+\sigma_2+\sigma_3)$. In computations this surface is conveniently represented directly in terms of the stress invariants. However, it is desirable to have a parametric representation for graphics purposes. The polar representation is derived in the Appendix.

TRIAXIAL COMPRESSION AND TENSION

Many triaxial tests are carried out with two of the three principal stresses equal. The results of these tests are conveniently described in terms of the mean stress σ_m and the difference between the largest and smalest principal stress. Let the principal stresses be ordered such that $\sigma_1 \geq \sigma_2 \geq \sigma_3$. The difference between the principal stresses is then characterized by

$$q = \sigma_1 - \sigma_3 \tag{9}$$

There are two types of test: triaxial compression and triaxial tension. In triaxial compression $\sigma_1 = \sigma_2 > \sigma_3$, and

$$\sigma_m = \tfrac{2}{3}\sigma_1 + \tfrac{1}{3}\sigma_3 \quad , \quad (s_1, s_2, s_3) = (\tfrac{1}{3}q_c, \tfrac{1}{3}q_c, -\tfrac{2}{3}q_c) \tag{10}$$

where the corresponding value of q on the deviatoric contour is denoted q_c. Similarly in triaxial tension $\sigma_1 > \sigma_2 = \sigma_3$, and

$$\sigma_m = \tfrac{1}{3}\sigma_1 + \tfrac{2}{3}\sigma_3 \quad , \quad (s_1, s_2, s_3) = (\tfrac{2}{3}q_t, -\tfrac{1}{3}q_t, -\tfrac{1}{3}q_t) \tag{11}$$

where q_t is the value of q on the deviatoric contour corresponding to triaxial tension. The location of the points of triaxial compression and tension on the deviatoric contour are shown in Fig. 4. Each of these points is reproduced three times by symmetry. It is commonly found that $q_c > q_t$, and convexity then requires $q_t > \frac{1}{2}q_c$.

For triaxial compression and tension the deviatoric stress invariants are

$$J_2^c = \tfrac{1}{3}q_c^2 \quad , \quad J_3^c = -\tfrac{2}{27}q_c^3 \tag{12}$$

and

$$J_2^t = \tfrac{1}{3}q_t^2 \quad , \quad J_3^t = \tfrac{2}{27}q_t^3 \tag{13}$$

Substitution of these expressions into the equation (8) for the deviatoric contour gives the following explicit expressions for the parameters of that equation.

$$\frac{1}{s_0^2} = \frac{3}{q_c^2\, q_t^2}\,\frac{q_c^3 + q_t^3}{q_c + q_t} = 3\,\frac{q_c^2 - q_c q_t + q_t^2}{q_c^2\, q_t^2} \tag{14}$$

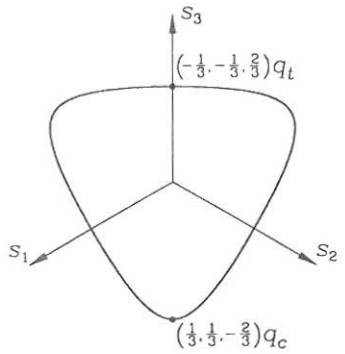

FIG. 4: Points of triaxial compression q_c and tension q_t.

$$\frac{\gamma}{s_0^3} = \frac{27}{2\,q_c^2\,q_t^2}\,\frac{q_c^2-q_t^2}{q_c+q_t} = \frac{27}{2}\,\frac{q_c-q_t}{q_c^2\,q_t^2} \tag{15}$$

The parameters s_0 and γ can now be eliminated from the equation (8) for the surface giving the equation

$$f(\sigma_1,\sigma_2,\sigma_3) = 27(q_c-q_t)\,J_3 + 6(q_c^2-q_cq_t+q_t^2)\,J_2 - 2\,q_c^2\,q_t^2 = 0 \tag{16}$$

where the triaxial compressive stress q_c and tensile stress q_t are given functions of th mean stress σ_m, i.e. $q_c = q_c(\sigma_m)$ and $q_t = q_t(\sigma_m)$. Specific surfaces obtained from linear o quadratic functions $q_c(\sigma_m)$ and $q_t(\sigma_m)$ are discussed below.

If the surface is described in terms of the size and shape parameters s_0 and γ the compres sion and tension generators q_c and q_t follow from solution of the cubic equation (8) afte substitution of (12) or (13). The solution follows directly from the polar representation o the Appendix as

$$q_c = \frac{s_0}{\cos\left(\frac{1}{3}\arccos(\gamma)\right)} \quad , \quad q_t = \frac{s_0}{\cos\left(\frac{1}{3}\arccos(-\gamma)\right)} \tag{17}$$

With the present sign convention for stresses $\gamma \geq 0$, and thus $q_c \geq q_t$.

THE PLANE STRESS CONTOUR

Before turning to specific models the plane stress contour is considered. Let the stress com ponents σ_1 and σ_2 be arbitrary, while $\sigma_3 = 0$. This enables a two-dimensional description

in terms of the mean stress σ_m and the stress difference $\Delta\sigma$,

$$\sigma_m = \tfrac{1}{3}(\sigma_1 + \sigma_2) \quad , \quad \Delta\sigma = \sigma_1 - \sigma_2 \tag{18}$$

In terms of these variables the deviatoric stress components are

$$s_1 = \tfrac{1}{2}(\sigma_m + \Delta\sigma) \ , \ s_2 = \tfrac{1}{2}(\sigma_m - \Delta\sigma) \ , \ s_3 = -\sigma_m \tag{19}$$

Substitution of these expressions into the deviatoric stress invariants J_3 and J_2 gives

$$J_3 = -\tfrac{1}{4}\sigma_m(\sigma_m^2 - \Delta\sigma^2) \quad , \quad J_2 = \tfrac{1}{4}(3\sigma_m^2 + \Delta\sigma^2) \tag{20}$$

The plane stress contour can now be obtained by substitution of these expressions into (16), whereby an equation for $\Delta\sigma^2$ is obtained. For any permissible value of σ_m the stress difference $\Delta\sigma$ is obtained from

$$\Delta\sigma^2 = \frac{8q_c^2q_t^2 - 18(q_c^2 - q_cq_t + q_t^2)\sigma_m^2 + 27(q_c - q_t)\sigma_m^3}{6(q_c^2 - q_cq_t + q_t^2) + 27(q_c - q_t)\sigma_m} \tag{21}$$

The limits on the mean stress σ_m in this formula are determined by the points corresponding to biaxial compression and biaxial tension.

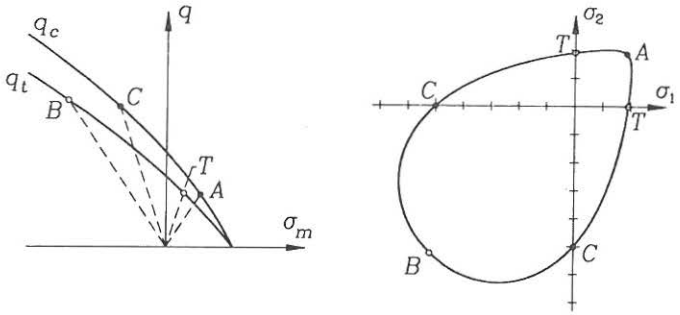

FIG. 5: Characteristic points of uniaxial and biaxial stress.

The general shape of the plane stress contour is characterised by four points A, B, C and T defined in Table 1 and shown in Fig. 5. They correspond to biaxial tension, biaxial compression, uniaxial compression and uniaxial tension. The location of these points on the compression and tension generators of the surface is indicated in Fig. 5a. The biaxial states are located on lines with inclination $q/\sigma_m = 3/\pm 2$, while the uniaxial states are located on the lines $q/\sigma_m = 3/\pm 1$. Note that biaxial compression is located on the

TABLE 1: Characteristic uniaxial and biaxial stress states.

	Point	(σ_1, σ_2)	σ_m	q
Biaxial tension	A	(σ_a, σ_a)	$\frac{2}{3}\sigma_a$	σ_a
Biaxial compression	B	$(-\sigma_b, -\sigma_b)$	$-\frac{2}{3}\sigma_b$	σ_b
Uniaxial compression	C	$(-\sigma_c, 0)$, $(0, -\sigma_c)$	$-\frac{1}{3}\sigma_c$	σ_c
Uniaxial tension	T	$(\sigma_t, 0)$, $(0, \sigma_t)$	$\frac{1}{3}\sigma_t$	σ_t

tension generator, while biaxial tension is loacted on the compression generator. Clearly the interval covered by the mean stress in the plane stress contour is determined by th biaxial states A and B, i.e. $-\frac{2}{3}\sigma_b < \sigma_m < \frac{2}{3}\sigma_a$.

The shape of the stress surface is to a large extent determined by the biaxial and uniaxia stress states A, B, C and T. In the following two sections the relation between these point and the parametric representation of the functions $q_c(\sigma_m)$ and $q_t(\sigma_m)$ is investigated fo linear and quadratic functions.

LINEAR GENERATORS

The simplest type of stress surface of the form (16) is generated by linear functions $q_c(\sigma_m$ and $q_t(\sigma_m)$. As a consequence of the convexity requirement these functions must intersec the hydrostatic axis in the same point, $\sigma_m = \sigma_0$. The linear functions can then be given i terms of σ_0 and two non-dimensional parameters α and β in the form

$$q_c(\sigma_m) = 3\,\alpha\,(\sigma_0 - \sigma_m) \quad , \quad q_t(\sigma_m) = 3\,\beta\,(\sigma_0 - \sigma_m) \tag{22}$$

where convexity requires $2\beta \geq \alpha$. This stress surface has stress contours with constan shape parameter,

$$\gamma = \frac{3\sqrt{3}}{2}\,\frac{(\alpha - \beta)\alpha\beta}{(\alpha^2 - \alpha\beta + \beta^2)^{3/2}} \tag{23}$$

This stress surface is illustrated in Fig. 6.

For $\alpha = \beta$ the surface is a circular cone. This is the Drucker-Prager stress surface, Drucke & Prager (1952). It is often used as a first approximation to the yield surface of materials with mean stress dependence due to its simple form. However, a stress surface with $\beta < \alpha$ will generally represent actual material behavior better.

If the three parameters α, β and σ_0 have been determined the four characteristic stress states A, B, C, and T follow immediately by substitution of the definitions from Table 1 into (22).

$$\sigma_a = \frac{3\alpha}{1+2\alpha}\sigma_0 \;,\; \sigma_b = \frac{3\beta}{1-2\beta}\sigma_0 \;,\; \sigma_c = \frac{3\alpha}{1-\alpha}\sigma_0 \;,\; \sigma_t = \frac{3\beta}{1+\beta}\sigma_0 \tag{24}$$

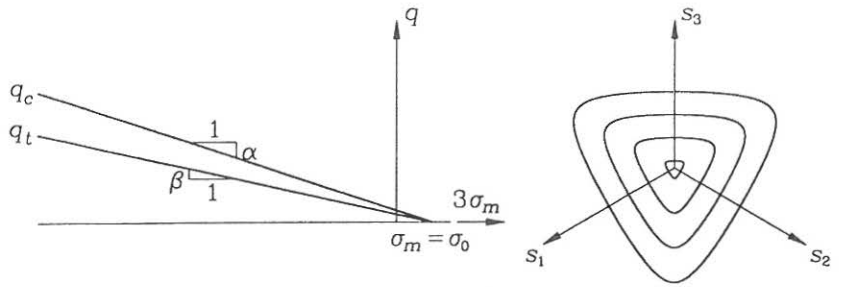

FIG. 6: Linear stress surface generators and deviatoric contours, $\alpha = 1/3$, $\beta = 2/9$.

Clearly a finite value of the uniaxial and biaxial compressive stress σ_c and σ_b requires $\alpha \leq 2\beta < 1$.

Conversely, the parameters α, β and σ_0 can be determined from any three of the characteristic stresses σ_a, σ_b, σ_c, and σ_t. Elimination of α and β in (24) establishes the following two equations

$$\frac{1}{\sigma_0} = \frac{1}{\sigma_a} - \frac{1}{\sigma_c} = \frac{1}{\sigma_t} - \frac{1}{\sigma_b} \tag{25}$$

These equations determine σ_0 and the fourth reference stress. The parameters α and β then follow from

$$\alpha = \frac{\sigma_c}{3\sigma_0 + \sigma_c} = \frac{\sigma_a}{3\sigma_0 - 2\sigma_a} \tag{26}$$

and

$$\beta = \frac{\sigma_b}{3\sigma_0 + 2\sigma_b} = \frac{\sigma_t}{3\sigma_0 - \sigma_t} \tag{27}$$

These formulae enable calibration in terms of three stresses. Naturally the biaxial shear stress can also be used as one of these stress values, but the corresponding formulae are slightly more indirect. The present formulation does not impose any restriction on the parameters, except those needed for convexity. This is an important advantage over other formats, e.g. that of Hibbitt et al. (1992) for granular materials, that only retain convexity in part of the parameter interval.

The general form of the stress surface with linear generators is described in terms of three parameters. However, there is an important class of materials for which the compression and tension generators are linked. This is the class of materials in which strength derives from a combination of cohesion and friction. In the linear case the strength of these materials is governed by the Mohr-Coulomb criterion

$$\tfrac{1}{2}(\sigma_1 - \sigma_3) + \tfrac{1}{2}(\sigma_1 + \sigma_3)\sin\varphi - c\cos\varphi = 0 \tag{28}$$

where σ_1 is the largest and σ_3 the smallest principal stress, while c is the cohesion and φ is the angle of friction, see e.g. Chen & Han (1988). When used as a plastic potential the angle of friction φ is replaced by the angle of dilatation ψ. The Mohr-Coulomb criterion is independent of the intermediate principal stress σ_2. The Mohr-Coulomb criterion gives a hexagonal contour in the deviatoric plane with corners on the compression and tension generators. Alternatively the stress surface (16) can be calibrated such that it coincides with the Mohr-Coulomb surface along the compression and tension generators. This offers computational advantages by smoothing the surface.

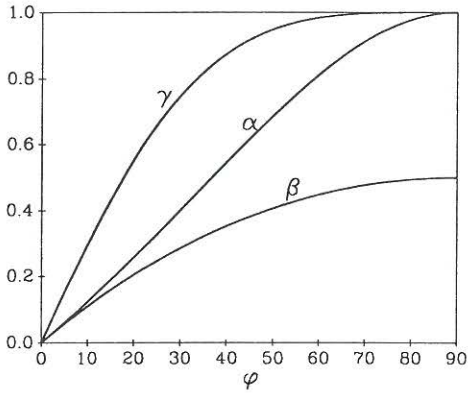

FIG. 7: Coefficients α, β and γ as function of friction angle φ.

Following the notation introduced in (9) the difference betwen the maximum and minimum principal stress is denoted $q = \sigma_1 - \sigma_3$. On the compression generator $\sigma_1 = \sigma_2 > \sigma_3$. This gives the relation

$$\sigma_1 + \sigma_3 \;=\; 2\sigma_m \;-\; \tfrac{1}{3}q \tag{29}$$

and thus the compression generator of the Mohr-Coulomb criterion takes the form

$$q_c(\sigma_m) \;=\; \frac{6\,\sin\varphi}{3-\sin\varphi}\,(c\,\cot\varphi \;-\; \sigma_m) \tag{30}$$

Similarly the stress states on the tension generator satisfy $\sigma_1 > \sigma_2 = \sigma_3$, whereby

$$\sigma_1 + \sigma_3 \;=\; 2\sigma_m \;+\; \tfrac{1}{3}q \tag{31}$$

This gives the tension generator of the Mohr-Coulomb criterion in the form

$$q_t(\sigma_m) \;=\; \frac{6\,\sin\varphi}{3+\sin\varphi}\,(c\,\cot\varphi \;-\; \sigma_m) \tag{32}$$

These generators are recognized as a special form of (22) with the three parameters given in terms of the angle of friction and the cohesion as

$$\alpha \;=\; \frac{2\,\sin\varphi}{3-\sin\varphi} \qquad , \qquad \beta \;=\; \frac{2\,\sin\varphi}{3+\sin\varphi} \tag{33}$$

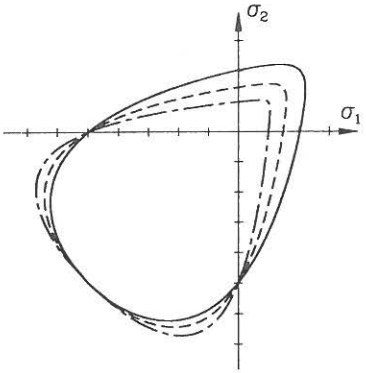

FIG. 8: Plane stress contours for interpolated Mohr-Coulomb material for $\sigma_t/\sigma_c = 0.2, 0.3, 0.4$ corresponding to $\varphi = 42°, 33°, 25°$.

and

$$\sigma_0 = c \cot \varphi \tag{34}$$

Note that the Mohr-Coulomb criterion corresponds to the condition

$$\frac{1}{\beta} - \frac{1}{\alpha} = 1 \tag{35}$$

The coefficients α and β are shown as function of the friction angle φ in Fig. 7. Both the coefficients approach their theoretical maximum value for φ aproaching 90°.

The shape coefficient of the smoothed Mohr-Coulomb surface is a constant defined in terms of the angle of friction as

$$\gamma = \frac{(3 + \sin\varphi)(3 - \sin\varphi)\sin\varphi}{(3 + \sin^2\varphi)^{3/2}} \tag{36}$$

The shape coefficient is shown as a function of the angle of friction in Fig. 7. It is seen that the full interval $0 \leq \gamma \leq 1$ is covered. The corresponding deviatoric contours can be seen in Fig. 3.

The two parameters of the Mohr-Coulomb criterion are determined from the uniaxial compression and tension stress.

$$\sin\varphi = \frac{\sigma_c - \sigma_t}{\sigma_c + \sigma_t} \quad , \quad \sigma_0 = \frac{\sigma_c \sigma_t}{\sigma_c + \sigma_t} \tag{37}$$

Figure 8 shows the plane stress contour for three interpolated Coulomb materials with linear generators. The tension part of these contours generally give too high stresses for actual materials. The Mohr-Coulomb surface with straight generators is therefore often

used in connection with a tension cut-off. An alternative is the use of surfaces with curved compression and tension generators. Two types of such surfaces are considered in the following sections.

The tension cut-off, also known as the Rankine criterion, can be expressed as

$$\sigma_1 \;=\; \max_j \sigma_j \;\leq\; \sigma_0 \tag{38}$$

Clearly, this is a limiting form of the Mohr-Coulomb criterion (28). The corresponding compression and tension generators are

$$q_c(\sigma_m) \;=\; 3(\sigma_m - \sigma_0) \qquad , \qquad q_t(\sigma_m) \;=\; \tfrac{3}{2}(\sigma_m - \sigma_0) \tag{39}$$

i.e. $\alpha = 2\beta = 1$. The deviatoric contour of the Rankine criterion is a triangle. Experimental results for such materials as concrete, rock and granular media suggest the use of the Rankine criterion as a limiting failure criterion for $\sigma_m \simeq \sigma_0$. A general convex failure criterion for these materials can therefore be expcted to satisfy the conditions

$$q_c(\sigma_m) \;\leq\; 2\,q_t(\sigma_m) \;\leq\; 3(\sigma_m - \sigma_0) \tag{40}$$

with equality being approached for $\sigma_m \simeq \sigma_0$.

QUADRATIC GENERATORS

A more general set of surfaces is obtained by using quadratic functions for the compression and tension generators. If the generators are assumed to be open for large negative values of the mean stress σ_m, i.e. not to intersect the negative hydrostatic axis, the general format is

$$\sigma_0 - \sigma_m \;=\; \frac{q^2}{a} \;+\; \kappa\, q \tag{41}$$

This is a quadratic parabola with axis parallel to the hydrostatic axis given by the three parmeters σ_0, a and κ, illustrated in Fig. 9. The apex of the parabola is located at the point

$$(\sigma_m, q)_{apex} \;=\; (\sigma_0 + \tfrac{1}{4}\kappa^2 a\,,\; -\tfrac{1}{2}\kappa a) \tag{42}$$

The stress parameter σ_0 is the intersection with the hydrostatic stress axis. This parameter must be common for the compresion and tension generators. The non-dimensional parameter κ is the slope of the generator at the intersection point,

$$\kappa \;=\; -\left.\frac{d\sigma_m}{dq}\right|_{q=0} \tag{43}$$

Clearly this slope must be positive, $\kappa > 0$. Furthemore this slope will typically be different for the compression and the tension generator, and the two values are denoted κ_c and κ_t, respectively. Convexity of the surface at this point requires $\kappa_t \leq 2\kappa_c$, where $\kappa_t = 2\kappa_c$

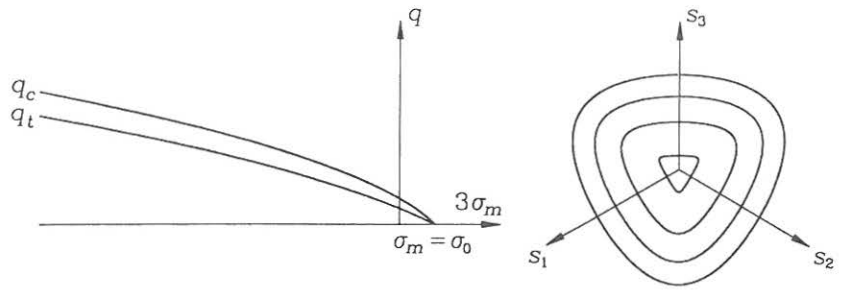

FIG. 9: Quadratic stress surface generators and deviatoric stress contours, $a/\sigma_0 = 50/3, 2\kappa_c = \kappa_t = 1/3$.

corresponds to a limiting triangular shape of the deviatoric stress contour when approaching zero size at $\sigma_m = \sigma_0$. The parameter a, with dimension of stress, determines the shape of the generator for large negative mean stress. If the deviatoric contour is assumed to approach circular shape for large negative mean stress the parameter a is the same for the compression and the tension generator.

Stress surfaces with quadratic compression and tension generators have been used extensively as failure criteria for concrete. Thus Bresler & Pister (1958) generalized the Drucker-Prager surface by introducing a quadratic generator, while retaining circular deviatoric contours. Other failure surfaces with different quadratic compression and tension generators have been proposed by Willam & Warnke (1975), Ottosen (1977), and Hsieh et al. (1982). These surfaces differ in the way the deviatoric contour is obtained from the compression and tension generators. Willam & Warnke (1975) interpolate in the 60° sectors between the generators in the deviatoric plane by using part of an ellipse. This is expressed in a rather complicated polar format. Ottosen (1977) assumes that *all* generators are parabolas generated by letting the coefficient of the linear term in q depend on the angle of the generator. Also this scheme leads to a polar representation of the deviatoric plane. The dependence of the coefficient κ on the angle in the deviatoric plane corresponds to that described in the Appendix for the present format. In the Hsieh-Ting-Chen surface the $\pm 60°$ sectors of the deviatoric plane are interpolated by parabolas with apex at the tension generator, Hsieh et al. (1982). This leads to corners at the compression generator. A survey of these three surfaces has been given by Chen & Han (1988).

A surface with quadratic compression and tension generators given by (41) with parameters σ_0, a, κ_c and κ_t is conveniently calibrated by data points $(\sigma_{m,c}, q_c)$ on the compression generator and points $(\sigma_{m,t}, q_t)$ on the tension generator. The general format for the parameter

TABLE 2: Parameters for concrete failure surfaces.

	σ_0/σ_c	a/σ_c	κ_c	κ_t
Hsieh-Ting-Cheng	0.1017	14.673	0.3669	0.6767
Willam-Warnke	0.1025	14.735 16.484	0.3680	0.6861
Ottosen	0.0965	9.645	0.3261	0.6209
$\kappa_t = 2\kappa_c$	0.0950	7.915	0.3020	0.6040
$\kappa_t = \frac{2}{3}$, $\kappa_c = \frac{1}{3}$	0.1010	9.900	0.3333	0.6666

calibration is

$$\begin{matrix} \textit{compression} \\ \textit{tension} \end{matrix} \left\{ \begin{bmatrix} 1 & -q_c^2 & -q_c & 0 \\ \vdots & \vdots & \vdots & \vdots \\ 1 & -q_t^2 & 0 & -q_t \\ \vdots & \vdots & \vdots & \vdots \end{bmatrix} \begin{bmatrix} \sigma_0 \\ 1/a \\ \kappa_c \\ \kappa_t \end{bmatrix} = \begin{bmatrix} \sigma_{m,c} \\ \vdots \\ \sigma_{m,t} \\ \vdots \end{bmatrix} \right. \tag{44}$$

The parameters can be determined directly by four data points or by a weighted least squares procedure if there are more than four points.

Table 2 shows parameters obtained for the failure surface of concrete on the basis of data from the literature. The parameters for the Willam-Warnke and the Hsieh-Ting-Chen surfaces are from the calibration by Chen & Han (1988) using $\sigma_t/\sigma_c = 0.10$, $\sigma_b/\sigma_c = 1.15$ and a representative point in triaxial compression. The parameters of the Ottosen surface are obtained from data of Schickert & Winkler (1977) using $\sigma_t/\sigma_c = 0.10$, $\sigma_b/\sigma_c = 1.21$ and a representative point in triaxial compression. The three calibrated surfaces all show nearly triangular shape of the deviatoric contour for $\sigma_m \simeq \sigma_0$, indicated by the ratio $\kappa_t/\kappa_c = 1.84, 1.86, 1.90$, respectively. The value 2 is the theoretical upper limit corresponding to a triangle. The table also contains parameters obtained by assuming exact triangular shape of the limiting deviatoric contour for $\sigma_m \simeq \sigma_0$, combined with $\sigma_t/\sigma_c = 0.10$, $\sigma_b/\sigma_c = 1.15$.

Figure 10 shows the plane stress contours corresponding to three different sets of parameters from Table 2. The exterior curve corresponds to the parameters of Ottosen, while the interior curve corresponds to the surface with limiting triangular shape $\kappa_t = 2\kappa_c$. The intermediate curve corresponds to the Hsieh-Ting-Chen parameters. It is seen that the effect of introducing the constraint $\kappa_t = 2\kappa_c$ is to contract the curve based on the original Hsieh-Ting-Chen parameters around $\sigma_1/\sigma_2 \simeq -1/-0.5$.

The compression and tension generators of the quadratic representation bear a simple relation to the Coulomb hypothesis of independence of the middle principal stress. If this hypothesis is valid, the compression and tension generators should produce the same curve

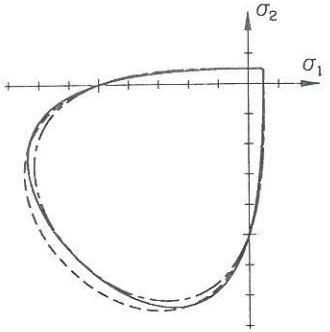

FIG. 10: Plane stress contours for quadratic generators.

when expressed in terms of $\frac{1}{2}(\sigma_1 + \sigma_3)$ and $q = (\sigma_1 - \sigma_3)$. On the generators this implies $\sigma_m = \frac{1}{2}(\sigma_1 + \sigma_3) \pm \frac{1}{6}q$. Thus the Coulomb hypothesis for the generators is equivalent to the condition

$$\kappa_t - \kappa_c = \frac{1}{3} \tag{45}$$

This condition implies that $\sigma_b = \sigma_c$ and $\sigma_a = \sigma_t$.

If the Rankine tension cut-off is imposed on the limition behavior of the generators for $\sigma_m \simeq \sigma_0$ the deviatoric contour, the linear terms are given explicitly by $\kappa_c = \frac{1}{3}$ and $\kappa_t = \frac{2}{3}$. A surface with quadratic generators that satisfy a limiting Rankine condition in tension may be calibrated entirely in terms of the two uniaxial stresses σ_c and σ_t.

$$\frac{a}{\sigma_c} = \frac{\sigma_c}{\sigma_t} - \frac{\sigma_t}{\sigma_c} \quad , \quad \sigma_0 a = \sigma_c^2 \tag{46}$$

The corresponding parameters for $\sigma_t/\sigma_c = 0.10$ have also been included in Table 2.

THE TWO-PARAMETER SURFACE OF LADE

A simple invariant stress surface with only two independent parameters was proposed by Lade (1977) as failure criterion and plastic potential for cohesionless soils. This surface turns out to be a particularly simple version of the general format (8) in which the deviatoric contour changes from complete triangular shape at zero mean stress to a circle for large compressive stress.

The original format of Lade's stress surface with the present sign convention for the stresses is

$$\left(\frac{I_1^3}{I_3} - 27\right)\left(\frac{-I_1}{p_a}\right)^m = \eta \tag{47}$$

where p_a is a reference pressure - taken as atmospheric pressure - while m and η are th parameters of the surface. The surface is expressed in terms of the Cauchy invariants fo the total stress

$$I_1 = \sigma_1 + \sigma_2 + \sigma_3 \quad , \quad I_3 = \sigma_2\sigma_3 + \sigma_3\sigma_1 + \sigma_1\sigma_2 \tag{48}$$

The total stress invariants I_1 and I_3 can be expressed in terms of the mean stress σ_m an the deviatoric stress invariants J_2 and J_3 as

$$I_1 = 3\sigma_m \quad , \quad I_3 = J_3 - \sigma_m J_2 + \sigma_m^3 \tag{49}$$

The equation (47) for the surface is conveniently restated in terms of a reference stress σ and a parameter λ in the form

$$\left(\frac{\sigma_m^3}{I_3} - 1\right)\left(\frac{-\sigma_m}{\sigma_*}\right)^m = \frac{1}{\lambda} \tag{50}$$

After expressing the total stress invariant I_3 in terms of the deviatoric stress invariants th equation for the surface takes the form

$$-\frac{J_3}{\sigma_m} + J_2 = \frac{\sigma_m^2}{1 + \lambda(-\sigma_m/\sigma_*)^m} \tag{51}$$

This is a special case of the format (8) where the size and shape parameters are given by

$$s_0 = \frac{-\sigma_m}{\sqrt{1 + \lambda(-\sigma_m/\sigma_*)^m}} \quad , \quad \gamma = \frac{1}{\sqrt{1 + \lambda(-\sigma_m/\sigma_*)^m}} \tag{52}$$

In the present context σ_m is negative, and thus the size parameter s_0 is always positive.

The formulae (52) for the size and shape parameters lead to a simple geometric interpretation of the Lade surface. The size of the exterior triangle associated with the present format and shown in Fig. 2 is given as $c = s_0/\gamma = -\sigma_m$. Thus the external triangles of the Lade surface constitute a pyramid with $c = |\sigma_m|$. This pyramid corresponds to the Rankine tension cut-off criterion (39) with $\sigma_0 = 0$. The actual surface is located inside this pyramid with size determined by s_0. The shape of the deviatoric contour is determined by the size of s_0 relative to $|\sigma_m|$, and thus the deviatoric contour is triangular for $\sigma_m \simeq 0$ and becomes increasingly circular with increasing value of $|\sigma_m|$. This transition in shape is governed completely by the growth in size, which is controlled by the exponent m and the scaling factor λ. In the present format using deviatoric stress invariants the surface is easily translated along the hydrostatic stress axis by replacing the mean stress σ_m with $\sigma_m - \sigma_0$.

CONCLUSIONS

A family of invariant stress surfaces with potential application as failure surface, yield surface and plastic potential has been described. Any surface of the family is generated

by two functions $q_c(\sigma_m)$ and $q_t(\sigma_m)$ defining the compression and tension meridian, respectively. The surface is generated by interpolation in the deviatoric plane using a cubic polynomial in the deviatoric stresses. Isotropic invariance imposes symmetry conditions such that the cubic interpolation can be reduced to a linear combination of the deviatoric stress invariants J_2 and J_3. This format constitutes a simple generalization of the von Mises and Drucker-Prager surfaces to include dependence on the third stress invariant. The dependence on the third stress invariant is essential for the representation of failure and deformation characteristics of e.g. granular materials, concrete and rock.

The general format does not impose any particular functional form on the generating functions $q_c(\sigma_m)$ and $q_t(\sigma_m)$ apart from convexity of the curves and the deviatoric convexity requirement $\frac{1}{2}q_c(\sigma_m) \leq q_t(\sigma_m) \leq q_c(\sigma_m)$. When the compression and tension generators are identical the deviatoric contour is circular, and the von Mises, Drucker-Prager and Bresler-Pister surfaces are obtained from a constant, linear or quadratic generator, respectively. Many materials require the use of generators with $q_t(\sigma_m) \leq q_c(\sigma_m)$, leading to smooth triangular deviatoric contours. The relation between the generators and the plane stress contour has been discussed, and an explicit formula for the plane stress contour is derived.

The special cases of linear and quadratic generators have been dealt with in some detail, and the use of a Mohr-Coulomb relation between the generators and the Rankine tension cut-off as a limiting condition have been discussed. Various calibrations of a failure surface with quadratic generators for concrete have been presented, using available data. The failure surface is nearly triangular in tension and becomes increasingly more circular with increasing compression. However, the quadratic format of the generators does not lead to accurate determination of the limiting behavior in tension.

The invariant family of stress surfaces can be described either in terms of the compression and tension generators or in terms of a size and shape function. It is demonstrated that the Lade surface for cohesionless soils, usually stated in terms of total stress invariants, in fact is a particularly simple case of a representation in terms of size and shape. The surface is contained within a triangular pyramid in stress space corresponding to the zero-tension cut-off, and for any value of the mean stress the size and shape of the deviatoric contour follows from the corresponding triaxial shear stress. The closer the contour is to the circumscribing triangle, the more triangular its shape. This way of representing the surface may be of interest in the representation of combined yield and failure surfaces for materials like concrete. It is desirable that the yield surface approaches the failure surface at failure after hardening. However, recent results by Labbane et al. (1993) indicate that the yield surface should be less triangular, at least in the initial stages of hardening. Thus, it is not feasible simply to introduce the yield surface simply as a scaled version of the failure surface. The present formulation suggests a possible alternative, where the yield surface becomes gradually more triangular with increasing magnitude as illustrated by the family of curves in Fig. 2.

Acknowledgment It is a pleasure to acknowledge information from N.S. Ottosen on failure surfaces for concrete and support from the Danish Technical Research Council.

REFERENCES

Bresler, B. and Pister, K.S., Strength of concrete under combined stresses, *Journal of th American Concrete Institution*, Vol. 55, pp. 321–345, 1958.

Chen, W.F. and Han, D.J., *Plasticity for Structural Engineers*, Springer-Verlag, New York 1988.

Drucker, D.C. and Prager, W., Soil mechanics and plasticity analysis of limit design, *Quar terly of Applied Mathematics*, Vol. 10, pp. 157–165, 1952.

Hibbitt, Karlsson and Sorensen, *ABACUS, Users Manual, Ver. 5.2*, Vol. 1, Sect. 4.6.3.1 1992.

Hsieh, S.S., Ting, E.C. and Chen, W.F., A plasticity-fracture model for concrete, *Interna tional Journal of Solids and Structures*, Vol. 18, pp. 181–197, 1982.

Labbane, M., Saha, N.K. and Ting, E.C., Yielding criterion and loading function for con crete plasticity, *International Journal of Solids and Structures*, Vol. 30, pp. 1269–1288 1993.

Lade, P.V., Elasto-plastic stress-strain theory for cohesionless soil with curved yield sur faces, *International Journal of Solids and Structures*, Vol. 13, pp. 1019–1035, 1977.

Ottosen, N.S., A failure criterion for concrete, *Journal of the Engineering Mechanics Di vision, ASCE*, Vol. 103, EM 4, pp. 527–535, 1977.

Schickert, G. and Winkler, H., Results of test concerning strength and strain of concrete subjected to multiaxial compressive stress, *Deutscher Ausschuss für Stahlbeton*, Heft 277 Berlin, 1977.

Willam, K.J. and Warnke, E.P., Constitutive model for the triaxial behavior of concrete, *Seminar on Concrete Structures Subjected to Triaxial Stress, Paper III-1, Bergamo, Italy, May 1974. Proceedings of the International Association for Bridge and Structural Engi neers*, Vol. 19, 1975.

APPENDIX: POLAR REPRESENTATION

In this appendix the contours given by the invariant cubic polynomial (8) are expressed in polar form. Any point in the principal deviatoric plane can be described in terms of its components along the two orthonormal vectors $\mathbf{e}_x, \mathbf{e}_y$ shown in Fig. 1.

$$\mathbf{e}_x = \frac{1}{\sqrt{2}}(-1,1,0) \quad , \quad \mathbf{e}_y = \frac{1}{\sqrt{6}}(-1,-1,2) \tag{53}$$

The components of the principal deviatoric stress vector s in terms of this basis are

$$s_x = \mathbf{s} \cdot \mathbf{e}_x = \frac{1}{\sqrt{2}}(s_2 - s_1) \tag{54}$$

$$s_y = \mathbf{s} \cdot \mathbf{e}_y = \frac{1}{\sqrt{6}}(2s_3 - s_1 - s_2) = \sqrt{\tfrac{3}{2}}\, s_3 \tag{55}$$

where the condition of zero mean of the deviatoric stresses has been used in (55). These components are now resolved in polar components in the form

$$s_x = -s \sin\theta \quad , \quad s_y = s \cos\theta \tag{56}$$

where the angle θ is referred to the y-axis because this is normally the vertical axis. The length s of the principal deviatoric stress vector s is given by

$$s^2 = s_x^2 + s_y^2 = s_1^2 + s_2^2 + s_3^2 \tag{57}$$

while the polar angle θ is given by

$$\cos\theta = \frac{s_y}{s} = \sqrt{\frac{3}{2}}\frac{s_3}{s} \tag{58}$$

It is clear from the symmetry of the problem that the angle 3θ plays a natural role. By substitution of (58) into the well known trigonometric relation for $\cos 3\theta$ we obtain

$$\cos 3\theta = 4\cos^3\theta - 3\cos\theta = 3\sqrt{\frac{3}{2}}\frac{s_3}{s}\frac{2s_3^2 - s^2}{s^2} \tag{59}$$

and upon substitution of s from (57) and use of the zero sum condition for the deviatoric stresses we get the relation

$$\cos 3\theta = \frac{3\sqrt{3}}{2}\frac{J_3}{J_2^{3/2}} \tag{60}$$

This relation is now used to write the general formula (8) for the contours in the deviatoric plane as a polar relation between the radius r and $\cos 3\theta$.

$$\left(\frac{s_0}{s}\right)^3 - \frac{1}{2}\left(\frac{s_0}{s}\right) - \frac{\gamma\cos 3\theta}{3\sqrt{6}} = 0 \tag{61}$$

This cubic equation in s_0/s can be solved directly by scaling the variable such that the ratio between the coefficients of the first two terms is 4 to 3. The solution can then be obtained by the trigonometric formula already used in (59). The scaled form is

$$4\left(\sqrt{\frac{3}{2}}\frac{s_0}{s}\right)^3 - 3\left(\sqrt{\frac{3}{2}}\frac{s_0}{s}\right) = \gamma\cos 3\theta \tag{62}$$

The solution is obtained by the substitution

$$\sqrt{\frac{3}{2}}\frac{s_0}{s} = \cos\varphi \tag{6}$$

into (62), whereby

$$\cos 3\varphi = \gamma \cos 3\theta \tag{6}$$

This gives the final form of the polar representation of the contours in the form

$$\frac{s_0}{s} = \sqrt{\tfrac{2}{3}} \cos\left(\tfrac{1}{3}\arccos(\gamma \cos 3\theta)\right) \tag{6}$$

This coincides with a generic curve used for the linear term in the quadratic failure criteric proposed by Ottosen (1977) with the size parameter $K_1 = \sqrt{\frac{2}{3}}s_0^{-1}$ and the shape paramet $K_2 = \gamma$. While this formula provides a convenient means for drawing the contours, th direct formulation (8) or (16) in terms of the deviatoric invariants J_2 and J_3 is considerabl simpler to use in computations, and offers the possibility of explicit calibration by poin on the deviatoric axes.

ENGINEERING MECHANICS PAPERS

PAPER NO. 1: S. Krenk: *Constrained Lateral Buckling of I-Beam Gable Frames.* ISSN 0902-7513 R8923.

PAPER NO. 2: S. Krenk & H. Gluver: *Markov Models and Range Counting in Random Fatigue.* ISSN 0902-7513 R9010.

PAPER NO. 3: S. Krenk & L. Damkilde: *Models of Thin-Walled Beam Connections.* ISSN 0902-7513 R9022.

PAPER NO. 4: S. Krenk & L. Damkilde: *Warping of Joints in I-Beam Assemblages.* ISSN 0902-7513 R9038.

PAPER NO. 5: S. Krenk: *Energy Release Rate of Adhesive Joints.* ISSN 0902-7513 R9111.

PAPER NO. 6: J. Jönsson, S. Krenk & L. Damkilde: *The Semi-Loof Element for Plate Instability.* ISSN 0902-7513 R9122.

PAPER NO. 7: S. Krenk: *A General Format for Curved and Nonhomogeneous Beam Elements.* ISSN 0902-7513 R9125.

PAPER NO. 8: S. Krenk: *A Calibration Formula for Clip-Gauge Measurement of Crack Growth in Adhesive Joints.* ISSN 0902-7513 R9127.

PAPER NO. 9: J. Jönsson, S. Krenk & L. Damkilde: *A Hybrid Displacement Plate Element for Bending and Stability Analysis.* ISSN 0902-7513 R9208.

PAPER NO. 10: S. Krenk, S. Vissing & C. Vissing-Jørgensen: *A Finite Step Updating Method for Elasto-Plastic Analysis of Frames.* ISSN 0902-7513 R9224.

PAPER NO. 11: Z. Zembaty & S. Krenk: *On the Spatial Seismic Excitations and Response Spectra.* ISSN 0902-7513 R9236.

PAPER NO. 12: J. Mann & S. Krenk: *Fourier Simulation of a Non-Isotropic Wind Field Model.* ISSN 0902-7513 R9248.

PAPER NO. 13: O. Hededal & S. Krenk: *A Profile Solver in C for Finite Element Equations.* ISSN 0902-7513 R9301.

PAPER NO. 14: L. Damkilde, O. Høyer & S. Krenk: *A Direct Linear Programming Solver in C for Structural Applications.* ISSN 0902-7513 R9304.

PAPER NO. 15: S. Vissing & S. Krenk: *A Generalized Jacobi Algorithm.* ISSN 0902-7513 R9316.

PAPER NO. 16: S. Krenk, L. Damkilde & O. Høyer: *Limit Analysis and Optimal Design of Plates with Triangular Equilibrium Elements.* ISSN 0902-7513 R9321.

PAPER NO. 17: S. Vissing & O. Hededal: *A Subspace Algorithm.* ISSN 0902-7513 R9322.

PAPER NO. 18: S. Krenk: *An Orthogonal Residual Procedure for Nonlinear Finite Element Equations.* ISSN 0902-7513 R9325.

ENGINEERING MECHANICS PAPERS

PAPER NO. 19: F. Mathiesen: *Stability Analysis of Thin-Walled Non-Symmetric Steel Beams.* Ph.D.-Thesis. ISSN 0902-7513 R9327.

PAPER NO. 20: J. Jønsson, S. Krenk & L. Damkilde: *Recursive Substructuring of Finite Elements.* ISSN 0902-7513 R9330.

PAPER NO. 21: S. Krenk & O. Hededal: *A Dual Orthogonality Procedure for Nonlinear Finite Element Equations.* ISSN 0902-7513 R9442.

PAPER NO. 22: S. Krenk: *A Family of Invariant Stress Surfaces.* ISSN 0902-7513 R9402.

Department of Building Technology and Structural Engineering
The University of Aalborg, Sohngaardsholmsvej 57, DK 9000 Aalborg
Telephone: 45 98 15 85 22 Telefax: 45 98 14 82 43